

Noise in the segmentation gene network of *Drosophila*, with implications for mechanisms of body axis specification

David M. Holloway^{*ab}, Lionel G. Harrison^b, Alexander V. Spirov^{cd}

^a Mathematics Department, British Columbia Institute of Technology, 3700 Willingdon Ave., Burnaby, B.C., Canada, V5G 3H2.

^b Department of Chemistry, University of British Columbia, 2036 Main Mall, Vancouver, B.C., Canada, V6T 1Z1.

^c Department of Applied Mathematics and Statistics, and Center for Developmental Genetics, State University of New York at Stony Brook, Stony Brook, New York, 11794-3600, USA.

^d The Sechenov Institute of Evolutionary Physiology and Biochemistry, Russian Academy of Sciences, 44 Thorez Ave., St. Petersburg, 194223, Russia.

ABSTRACT

Specification of the anteroposterior (head-to-tail) axis in the fruit fly *Drosophila melanogaster* is one of the best understood examples of embryonic pattern formation, at the genetic level. A network of some 14 segmentation genes controls protein expression in narrow domains which are the first manifestation of the segments of the insect body. Work in the New York lab has led to a databank of more than 3300 confocal microscope images, quantifying protein expression for the segmentation genes, over a series of times during which protein pattern is developing (<http://flyex.ams.sunysb.edu/FlyEx/>). Quantification of the variability in expression evident in this data (both between embryos and within single embryos) allows us to determine error propagation in segmentation signalling. The maternal signal to the egg is highly variable, with noise levels more than several times those seen for expression of downstream genes. This implies that error suppression is active in the embryonic patterning mechanism. Error suppression is not possible with the favoured mechanism of local concentration gradient reading for positional specification. We discuss possible patterning mechanisms which do reliably filter input noise.

Keywords: gene regulation, quantitative protein expression, error propagation, *Drosophila melanogaster*, embryonic axis specification, image processing, confocal microscopy, concentration noise, positional specification, spatial pattern formation.

1. INTRODUCTION

Positionally specific gene regulation is believed to be a fundamental process underlying embryological development, responsible for the patterned cell differentiation at the heart of many developmental events. Spatial pattern has long been thought to be specified by gradients^{1,2,3} more recently identified as gradients in concentration of regulators of differentiation (e.g. signalling molecules or transcriptional regulators). Wolpert^{4,5,6} has elaborated greatly on this idea, that cells acquire positional information (knowing where they are in the organism) by reading the local concentration of gradient molecules.

In the establishment of animal body plans, it is evident that the reading of relatively simple information such as a spatially monotonic gradient leads to more complex responses, e.g. formation of a pattern of stripes of gene expression (as RNA or proteins), which go on to command the formation, through many further gene-switchings, of appropriate body organs in the right places. The genetic interactions thus have a strongly sequential or hierarchical aspect, with more network-like behaviour to interpret the received information at each level of the hierarchy. Information is being conveyed by highly reactive molecules, that are capable of operating in small numbers, e.g. thousands^{7,8,9}, susceptible to expected concentration fluctuation errors of a few percent (Poisson basis). The question of noise levels in such

*David_Holloway@bcit.ca; phone 1 604 456-8199; fax 1 604 432-9173

information-transmitting and -processing systems is very important in relation to an ultimate response so intolerant of errors as an animal body plan.

In the early development of the fruit fly (*Drosophila melanogaster*), a gradient of the Bicoid (Bcd) protein, translated from maternally-deposited RNA, is established along the length of the egg⁷, with highest concentration at the anterior (head) end, and lowest concentration in the posterior (Fig 1A). Bcd is a transcriptional regulator, and lies at the top of a genetic hierarchy which results in the proper segmentation of the body plan in the anteroposterior (AP) axis. Bcd is cited as a prime example of positional specification by gradients^{10,11,7,12}: downstream segmentation genes are regulated by Bcd in a concentration dependent manner. The gap class of genes refine the input of the Bcd gradient, being expressed in domains with sharp spatial boundaries (Fig. 1B). These gap genes, in turn, regulate pair-rule class genes, giving narrow stripes of expression (Fig. 1C). Pair-rule pattern is the first manifestation of the segmented body plan characteristic of insects. Local reading of concentration gradients has generally been the favoured mechanism within this patterning hierarchy, but there are a number of proposals for pair-rule patterning (e.g.^{13,14,15,16,17}) and the question remains quite open.

The various proposed models can be evaluated in a descriptive sense: how well they mimic natural pattern; how well they model mutations; how well they respond to changes in embryo geometry. Models may also provide experimentally testable predictions regarding particular gene interactions¹⁵. Another avenue for model testing, and ultimately to understanding the natural segmentation mechanism, is to use noise as a tool to elucidate underlying gene dynamics.

A chief concern in such a concentration dependent regulatory network is what effects molecular-scale fluctuations (in reactions and transport) have on the system's ability to specify position precisely. The early transcriptional regulators in *Drosophila* are at low enough concentrations that relative errors should be significant. There are two aspects to using these fluctuations to probe gene dynamics: experimentally, the concentration fluctuations (or more specifically, their effects on positional specification) must be characterized; and theoretically, the proposed segmentation models must be shown robust to these levels of error.

Recent experimental analysis^{18,19,20} has begun to characterize the natural variability in segmentation gene expression. These studies demonstrate error suppression within the segmentation network: downstream genes show greater positional precision than the maternal Bcd gradient.

This has immediate implications for the favoured local gradient reading model of segmentation: Wolpert-style signalling has no capacity to suppress errors. The segmentation mechanism must contain error suppressing dynamics, perhaps of one of the types proposed in recent years^{21,22,23}.

There has been growing interest in the stochastic nature of gene regulation^{24,25,26,27,28,29}. The study of this within gene networks, theoretically and experimentally, has focused chiefly on bacterial systems. Our *Drosophila* data allows us to begin probing noise effects in a complex eukaryotic gene network, and using this to uncover the network kinetics.

In the present work, we do a detailed analysis at the top of the segmentation signalling hierarchy, that is, the positional errors of the maternally-derived Bcd gradient, and compare these with the theoretical predictions of Lacalli and Harrison³⁰. Their paper quantified the limits in precision for positional specification by an exponential Bcd gradient, based on propagation calculations for molecular-level errors in Bcd production, decay, and transport rates. Here, we present experimental profiles of fluorescence intensity (proportional to Bcd concentration) against AP position, extracted from whole embryo confocal microscope images, and compare variability in these with theoretical predictions. This allows for a full understanding of Bcd variability, in order to focus in future on the mechanism of error suppression in the downstream transmission of the Bcd message.

2. METHODS

2.1 Images of *Drosophila* Gene Expression

Protein concentration was measured using fluorescently-tagged antibodies as described in³¹. For each embryo a 1024 × 1024 pixel image with 8 bits of fluorescence intensity data in each of 3 channels was obtained (Fig. 1: parts A, B, and C

are from separate channels, visualizing three different proteins from the same embryo with one snapshot). Image processing³² transforms each image into an ASCII table containing a series of data records, one for each nucleus. About 2500-3500 nuclei are described for each image. Each nucleus is characterized by a unique identification number, the AP and dorsoventral (DV) coordinates of its centroid, and the average fluorescence intensities of three gene products. The overall result is the conversion of an image to a set of numerical data which is then suitable for further processing. There are currently over 3300 embryo images, with data on 14 segmentation genes, in the databank. Most of the raw images, details and results of image pre-processing, and the results from two image registration techniques are available on the Web bases *FlyEx* (<http://flyex.ams.sunysb.edu/FlyEx/>) and *Mooshka* (<http://urchin.spbcas.ru/Mooshka/>).

2.2 Temporal Classification

Embryos in the databank belong to nuclear cleavage cycles 10 to 14³³. In these cycles, the Bcd gradient is established and maintained. In cycle 14 (about an hour long), the finer-scale gap and pair-rule patterns develop. Within cycle 14, embryos were classified into eight time classes, primarily by visual inspection of the (highly dynamic) expression pattern of the pair-rule gene *Even-skipped*¹⁸ (all embryos were stained for Even-skipped protein, as well as two others). This classification was later verified by observation of other protein patterns and by membrane invagination data. In this paper, we are primarily concerned with characterizing Bcd error as it initiates the segmentation hierarchy. Therefore, we present data from the first time class of cycle 14, for which we have Bcd data from 52 embryos.

2.3 Extraction of the AP Bcd gradient

We are interested in characterizing the precision with which the Bcd gradient can specify position along the AP axis. Therefore, Bcd positional errors are calculated directly in terms of the variability of AP positions over which nuclei exhibit a particular fluorescence intensity range (rather than circumstantially, using Bcd intensity fluctuations). We calculate positional error both for between-embryo variability and for within-embryo variability. To get a large number of nuclei for these statistics, we use a significant portion, in the DV direction, of the original image. Use of such data is complicated by a slight DV dependence of AP pattern (evident in the stripe bending of Fig. 1C). We remove this dependence with a polynomial deformation of nuclear coordinates, which uses an evolutionary programming approach with a cost function based on the straightness of pair-rule stripes^{34,36}. This allows us to sample a rectangle of nuclei from each image, of 50% DV height, centred on the AP axis. This captures approximately 1400-1700 nuclei (cleavage cycle 14). Fig. 2 shows a scatterplot of fluorescence intensity for each nucleus against AP position, in percent egg length (% E.L.), for a single embryo. Between-embryo variability is calculated from the differences between averaged single-embryo profiles. Within-embryo variability is calculated directly off scatterplots like Fig. 2.

2.4 Quantification of positional errors

The intensity scale is divided into 36 equal-height bins. Within each bin, mean and standard deviation AP positions are calculated. These standard deviations are the within-embryo positional errors, giving estimates on variability due to molecular fluctuations in the mechanism establishing and maintaining the Bcd gradient (Fig. 4). For between-embryo positional error, standard deviations are calculated from the single-embryo means for each intensity bin (Fig. 3), giving estimates of embryo-to-embryo variability.

There is some concern that all of a standard deviation calculated as above may not be due to actual molecular fluctuations or between-embryo variability: part of the positional scatter of nuclei in an intensity bin serves to define the slope of the Bcd gradient, and this slope decreases exponentially towards the posterior. To see the effect of removing this slope contribution, we have also binned the data exponentially. That is, bin heights are decreased exponentially towards the posterior.

3. RESULTS AND DISCUSSION

Fig. 2 is a scatter plot of fluorescence intensity vs. AP position for a single embryo (early cleavage cycle 14). Each dot is the intensity for a single nucleus. From this, it is apparent there is a fair degree of scatter in positions for any given intensity interval. If Bcd is a morphogenetic gradient, positioning cell type along the AP axis by its concentration, a similar scatter should be seen, ultimately, in cell type, and earlier in the expression of downstream segmentation genes (addressed below, Fig. 5).

In 1991, Lacalli and Harrison³⁰ predicted that this positional scatter should increase towards the posterior of the embryo. Their analysis was based upon calculations of the contributions of molecular scale fluctuations to positional error for an exponential Bcd gradient in 1D. An exponential concentration (C) gradient along AP position s

$$C = C_0 e^{-\sqrt{k/D}s} \quad (1)$$

can be set up by a local source of Bcd protein (C_0) at the anterior pole, followed by diffusion into the embryo (with diffusivity D) and first-order degradation of the protein throughout (rate constant k). (The assumption of a 1D exponential fits the experimental data well, e.g.¹⁹, but we are currently investigating deviations from the exponential due to diffusion in the 2D shell of surface nuclei or the full 3D embryo.) Molecular fluctuations can affect the shape of the exponential through either C_0 or k/D . Lacalli and Harrison³⁰ showed that C_0 gives homogeneous contributions to positional error

$$\sigma_{s_{C_0}} = \sqrt{D/k} \delta C_0 \quad (2)$$

(where $\sigma_{s_{C_0}}$ is the absolute error (standard deviation) in s due to the relative error in C_0 , $\delta C_0 = \sigma C_0 / C_0$), while k/D contributions rise linearly towards the posterior

$$\sigma_{s_{(k/D)}} = (s/2) \delta (k/D) \quad (3)$$

(where $\sigma_{s_{(k/D)}}$ is the absolute error in s due to the relative error in k/D , $\delta (k/D) = \sigma (k/D) / (k/D)$).

Here, we test these theoretical predictions against the positional errors found in real Bcd gradients. Fig. 3A shows the between-embryo statistics (see section 2.4 for details) for 52 Bcd profiles. Mean positions and 1 standard deviation error bars are shown for each intensity bin. This shows a trend of increasing positional error (standard deviation) towards the posterior of the embryo (Fig. 3B). In Fig. 3B, the minimum (leftmost) value can be taken as the homogeneous C_0 contribution, shared by all positions. This value, roughly 1.6 standard deviations (units of %EL), translates into roughly 7% relative error in C_0 (using eqn. 2, and an exponential decay constant of 4.5/EL for Fig. 3A). This is somewhat more than the 5% C_0 error used by Lacalli and Harrison³⁰ for their calculations, which they cited as too high to correlate with the robustness of real embryos. Error in C_0 can arise from a variable (between embryos) deposition of Bcd RNA by the mother on the anterior pole, and from molecular fluctuations (within embryos) affecting the translation rate of RNA to Bcd protein.

For the k/D fluctuations, we see a posteriorly rising component to the positional errors in Fig. 3B. Though there is some nonlinearity in this Figure, linear regression gives significant ($p < 0.01$) correlation, with $R^2 = 0.80$. This line has a slope of 8% and a y-intercept of 2.4 (which would give a higher estimate of C_0 error than above). From eqn. (3), this slope is half of the k/D error, giving an estimate of 16% for k/D error. This is slightly less than the 20% k/D error used in the calculations in^{30, Fig. 2}. k/D errors can arise from variability in enzyme concentrations and transport properties between embryos, and from molecular fluctuations in reactions and diffusion within embryos. We expect experimental errors (due to variability in embryo fixation, staining and antibody quality), though minimized, to have greatest effect on background, C_0 , noise rather than follow the spatial dependence of k/D errors.

With exponential binning, to remove slope contributions to the standard deviations, the trends remain very similar (Fig. 3C). A linear regression on these data has a slightly better fit ($R^2 = 0.82$), giving a slope of 9% and a y-intercept of 2.1. In Figs. 3C and 4B, an exponential base of 1.1 was used, giving 15 bins of between 50 and 100 nuclei each (a smaller range than with non-exponential binning). Trends were similar with other exponential bases, but the number of nuclei per bin was not as consistent.

We estimate the standard deviation of the exponential decay constant to be 0.36/EL. (The fractional positional error, the slope from Fig. 3B, is equal to the fractional error in the decay constant. The standard deviation for the decay constant is obtained by multiplying the value of $\sqrt{k/D}$ by the slope of Fig. 3B). This translates into a standard deviation of 0.018 EL for the reciprocal of the decay constant, slightly less than half the value of 0.045 EL recently reported in¹⁹.

We can focus on molecular sources of the C_0 and k/D contributions to positional error by doing statistics on single embryos, removing contributions from between-embryo and experimental variability. Here, we directly calculate

positional standard deviations in each intensity bin. Fig. 4A shows these positional errors vs. AP distance for equal-height intensity bins, showing a similar posteriorly rising trend to Fig. 3B. The background, C_0 , error is around 1 %EL, comparable to that seen in Fig. 3B. The trend is nonlinear, but generally reaches similar levels in the posterior as Fig. 3B, agreeing with the estimates for k/D error made from Fig. 3. Exponential binning for these data (Fig. 4B) appears to reduce the posterior rise in the positional errors (and increase the anterior noise). This may be an effect of the bin resolution and warrants further investigation.

From characterizing Bcd errors, a chief interest is to see how these errors are propagated downstream in the segmentation hierarchy. Previous studies have shown reduction of Bcd error in the downstream genes, at particular positions in the embryo^{19,20}. This has suggested that simple Wolpert-style reading of the Bcd gradient is insufficient for proper spatial expression of downstream genes. Here, we extend this conclusion to more positions in the embryo. Fig. 5 shows positional errors for the gap protein Hunchback (Hb; also in Fig. 1B), which is directly regulated by Bcd. By visual inspection, Hb errors are similar to, or worse than, Bcd errors (Fig. 4B) up to about 45 %EL, at which point Hb becomes fairly well controlled, with errors of roughly 1 %EL, as Bcd errors continue to climb. The slight posterior rise in Hb errors past about 60 %EL is still much lower than that of Bcd. The positioning of the sharp Hb boundary at about 50 %EL (see Fig. 1B) is biologically important, and it is in this region that Hb errors are clearly independent of the noisier upstream Bcd signal.

4. CONCLUSIONS

The chief focus of this paper was to test the predictions of Lacalli and Harrison³⁰ for positional error trends in Bcd signalling with our recent data on segmentation patterns. We have shown that Bcd positional errors do generally follow the trends predicted by error propagation of an exponential gradient. Estimated levels for exponential source (C_0) and decay (k/D) variability are high, comparable to values used in calculations by Lacalli and Harrison³⁰, which were considered large overestimations at the time. With such large Bcd errors, the question becomes how does the fruit fly embryo reduce this noise to form a precisely patterned body plan? Preliminary work^{19,36,20} is showing that gap and pair-rule genes do have far lower positional error than Bcd. Experimental and data analysis work continues in order to characterize these errors, and use relative error levels to shine some light on the underlying kinetics in the segmentation mechanism. The initial results have shown that this mechanism is not solely reliant upon local reading of the Bcd gradient. Something a bit more complex is at work, and there exist some proposals for possible noise reducing mechanisms^{21,23,37,22}. These latter two works demonstrate the noise reduction inherent in Turing³⁸ reaction-diffusion dynamics. Turing models have been proposed for segmentation patterning, but experimental corroboration, for any model, remains difficult. We hope that accurate response to experimentally-characterized noise levels may become a point of testing for any proposed segmentation model.

ACKNOWLEDGEMENTS

We thank J. Reintz for stimulating discussions. AVS was supported by NIH RR07801, by INTAS grant No 97-30950 and by RFBR grant No 00-04-48515. LGH and DMH thank NSERC Canada for financial support. DMH thanks BCIT for travel funding.

REFERENCES

1. T. Boveri, *Ergebnisse über die Konstitution der chromatischen Substanz des Zellkerns*, Gustav Fischer, Jena, 1904.
2. T. Boveri, "Die Potenzen der *Ascaris*-Blastomeren bei abgeänderter Furchung, zugleich ein Beitrag zur Frage qualitative-ungleicher Chromosomen-Teilung" *Festschrift für Richard Hertwig*, 3, p. 131, Gustav Fischer, Jena, 1910.
3. K. Sander, "Of gradients and genes: developmental concepts of Theodor Boveri and his students", *Roux's Arch. Dev. Biol.*, **203**, 295-297, 1994.
4. L. Wolpert, "Positional information and the spatial pattern of cellular differentiation", *J. Theor. Biol.*, **25**, 1-47, 1969.
5. L. Wolpert, "Positional information and pattern formation", *Towards a Theoretical Biology*, C.H.Waddington, 3, p. 198, Edinburgh University, 1970.
6. L. Wolpert, "Positional information and pattern formation" *Curr. Top. Dev. Biol.*, **6**, 183-224, 1971.
7. W. Driever and C. Nüsslein-Volhard, "A gradient of *bicoid* protein in *Drosophila* embryos", *Cell* **54**, 83-93, 1988.

8. W. Driever and C. Nüsslein-Volhard, "The *bicoid* protein determines position in the *Drosophila* embryo in a concentration-dependent manner", *Cell*, **54**, 95-104, 1988.
9. J.B. Gurdon and P.-Y. Bourillot, "Morphogen gradient interpretation", *Nature*, **413**, 797-803, 2001.
10. L. Wolpert, *Principles of Development*, 2nd Ed., Oxford University Press, 2002.
11. S.F. Gilbert, *Developmental Biology*, 4th Ed., Sinauer, Sunderland, Mass., USA, 1994.
12. G. Struhl, K. Struhl, and P.M. Macdonald, "The gradient morphogen bicoid is a concentration-dependent transcriptional activator", *Cell*, **57**, 1259-1273, 1989.
13. H. Meinhardt, "Models for maternally supplied positional information and the activation of segmentation genes in *Drosophila* embryogenesis", *Development*, **104** (Suppl.), 95-110, 1988.
14. T.C. Lacalli, "Modeling the *Drosophila* pair-rule pattern by reaction-diffusion: gap input and pattern control in a 4-morphogen system", *J. Theor. Biol.*, **144**, 171-194, 1990.
15. J. Reinitz and D.H. Sharp, "Mechanism of formation of eve stripes", *Mech. of Dev.*, **49**, 133-158, 1995.
16. A. Hunding, "Supercomputer simulation of Turing structures in *Drosophila* morphogenesis", *Experimental and Theoretical Advances in Biological Pattern Formation*, H.G. Othmer et al., 149-159, Plenum Press, New York, 1993.
17. J.W. Bodnar, "Programming the *Drosophila* embryo", *J. Theor. Biol.*, **188**, 391-445, 1997.
18. E. Myasnikova, A. Samsonova, K. Kozlov, M. Samsonova, and J. Reinitz, "Registration of the expression patterns of *Drosophila* segmentation genes by two independent methods", *Bioinformatics*, **17**, 3-12, 2001.
19. B. Houchmandzadeh, E. Wieschaus, and S. Leibler, "Establishment of developmental precision and proportions in the early *Drosophila* embryo", *Nature*, **415**, 798-802, 2002.
20. A.V. Spirov and D.M. Holloway, "Making the body plan: precision in the genetic hierarchy of *Drosophila* embryo segmentation", *In Silico Biology*, **3**, 0009, 2003, <<http://www.bioinfo.de/isb/2003/03/0009/>>.
21. M. Kerszberg, "Accurate reading of morphogen concentrations by nuclear receptors: a formal model of complex transduction pathways", *J. Theor. Biol.*, **183**, 95-104, 1996.
22. D.M. Holloway and L.G. Harrison, "Suppression of positional errors in biological development", *Math. Biosc.*, **156**, 271-290, 1999.
23. M. Thattai, and A. van Oudenaarden, "Attenuation of noise in ultrasensitive signaling cascades", *Biophysical J.*, **82**, 2943-2950, 2002.
24. M.S.H. Ko, "A stochastic model for gene induction", *J. Theor. Biol.*, **153**, 181, 1991.
25. M.S.H. Ko, "Induction mechanism for a single gene molecule: stochastic or deterministic?", *BioEssays*, **14**, 341-346, 1992.
26. I.L., Ross, C.M., Browne, and D.A. Hume, "Transcription of individual genes in eukaryotic cells occurs randomly and infrequently", *Immunol. Cell Biol.*, **72**, 177-185, 1994.
27. H.H. McAdams and A. Arkin, "It's a noisy business!", *Trends in Genetics*, **15**, 65-69, 1999.
28. J. Hasty, J. Pradines, M. Dolnik, and J.J. Collins, "Noise-based switches and amplifiers for gene expression", *Proc. Nat. Acad. Sci. USA*, **97**, 2075-2080, 2000.
29. M. Thattai and A. van Oudenaarden, "Intrinsic noise in gene regulatory networks", *Proc. Nat. Acad. Sci. USA*, **98**, 8614-8619, 2001.
30. T.C. Lacalli and L.G. Harrison, "From gradients to segments: models for pattern formation in early *Drosophila* embryogenesis", *Semin. Dev. Biol.*, **2**, 107-117, 1991.
31. D. Kosman, S. Small and J. Reinitz, "Rapid preparation of a panel of polyclonal antibodies to *Drosophila* segmentation proteins", *Dev. Genes Evol.*, **208**, 290-294, 1998.
32. D. Kosman, J. Reinitz and D.H. Sharp, "Automated assay of gene expression at cellular resolution", *Proceedings of the 1998 Pacific Symposium on Biocomputing*, R. Altman et al., 6-17, World Scientific Press, Singapore, 1999.
33. V.A. Foe and B.M. Alberts, "Studies of nuclear and cytoplasmic behaviour during the five mitotic cycles that precede gastrulation in *Drosophila* embryogenesis", *J. Cell Sci.*, **61**, 31-70, 1983.
34. A.V. Spirov, A.B. Kazansky, D.L. Timakin, J. Reinitz, and D. Kosman, "Reconstruction of the dynamics of the *Drosophila* genes from sets of images sharing a common pattern", *J. Real-Time Imaging*, **8**, in press, 2002.
35. A.V. Spirov and D.M. Holloway, "Evolutionary techniques for image processing a large dataset of early *Drosophila* gene expression", *EURASIP Journal of Applied Signal Processing*, in press, 2003.
36. D.M. Holloway, J. Reinitz, A. Spirov, and C.E. Vanario-Alonso, "Sharp borders from fuzzy gradients", *Trends in Genetics*, **18**, 385-387, 2002.
37. A. Gierer and H. Meinhardt, "A theory of biological pattern formation", *Kybernetik*, **12**, 30-39, 1972.
38. A.M. Turing, "The chemical basis of morphogenesis", *Phil. Trans. R. Soc. Lond. B*, **237**, 37-72, 1952.

FIGURE LEGENDS

Figure 1: Confocal microscope images of a fruit fly embryo (roughly 0.5 mm long), stained with fluorescent antibodies to three different gene products (Bicoid, Hunchback and Even-skipped), in late cleavage cycle 14 (about 4 hours of development; see Foe and Alberts 1983, for *Drosophila* staging). At the beginning of the cycle, most of the nuclei (approximately 8000) are in a single layer at the surface of the egg (which is a multinucleate single cell, or syncytium). By the end of the cycle, membranes have grown inwards to enclose each nucleus separately, and create a sheet of cells. Fluorescence intensity is proportional to protein concentration. Anterior left, posterior right, dorsal up, ventral down. Each dot is a nucleus (approximately 3000 in view at this orientation, but not all will have high fluorescence for a particular protein). A) Stain for Bicoid (Bcd) protein, maternal class. B) Stain for Hunchback protein, gap class. C) Stain for Even-skipped protein, pair-rule class.

Figure 2: Fluorescence intensity vs. anteroposterior (AP) position, for a single embryo (early cleavage cycle 14) stained for Bicoid (Bcd) protein. Each point represents fluorescence intensity at a single nucleus. From stripe-straightened images, data was taken from 50% dorsoventral (DV) slices, giving a small sample of nuclei for each AP position, or (as used in this paper), increment in intensity.

Figure 3: For 52 early cycle 14 embryos: **A)** Mean AP positions, with 1 standard deviation (variation between embryos) error bars, for each (equal-height) intensity bin. **B)** Positional errors (the 1 standard deviation error bars from **A** against AP position for the same data. Regression line is shown. A posteriorly rising trend is observed, as predicted by Lacalli and Harrison (1991). From this, we estimate noise levels in the Bcd mechanism (see text). **C)** Same data, with exponentially decreasing intensity bin height (see section 2.4). Regression line is shown. Overall trends and Bcd noise estimates similar to **B**.

Figure 4: For the same 52 embryos: **A)** Positional error (within-embryo standard deviation) vs. AP position (compare Fig. 3B). Each line represents one embryo. Increasing error towards the posterior is still observed with individual embryos. **B)** Exponentially decreasing bin heights (as in Fig. 3C). The posterior rise in the errors appears reduced (and anterior noise increased).

Figure 5: Downstream reduction of Bcd noise. Positional error vs. AP position for 37 early cycle 14 embryos stained for the gap-class gene Hunchback (Fig. 1B). These are exponentially binned, as in Fig. 4B. Each line represents one embryo. Overall noise is less than for Hunchback's direct upstream regulator, Bcd (compare Fig. 4B), especially in the mid-embryo region, where an important boundary in Hunchback concentration is defined.

Figure 1

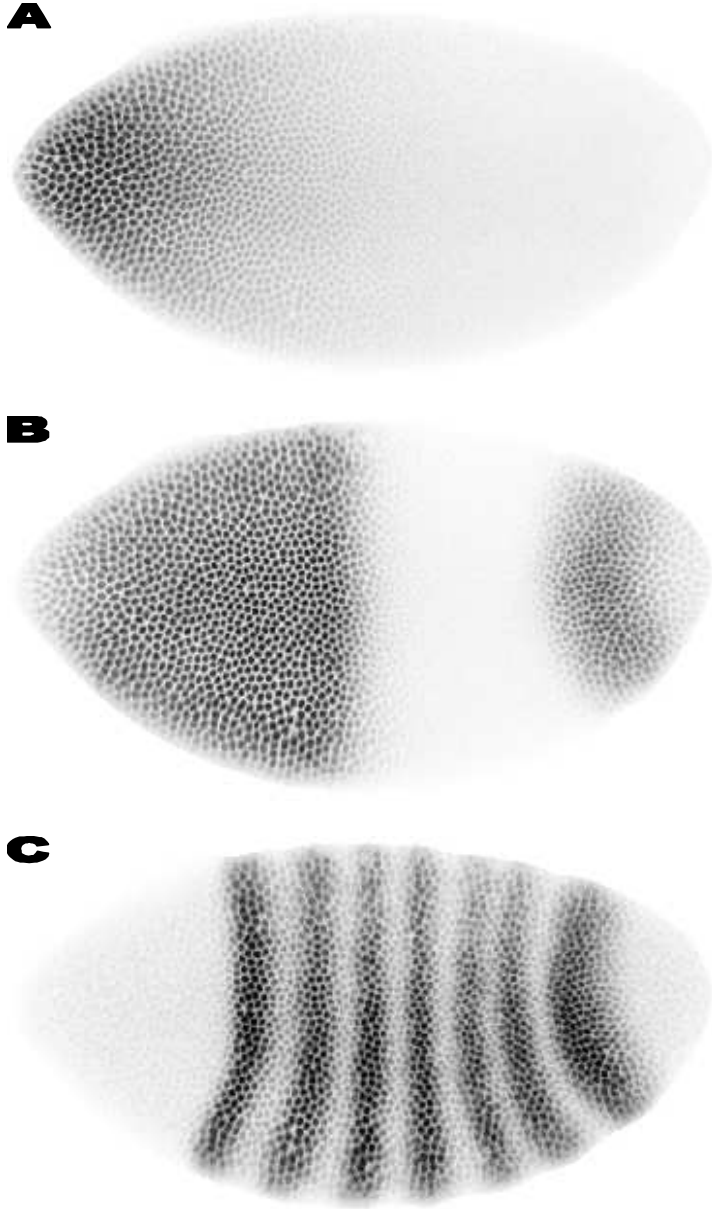


Figure 2

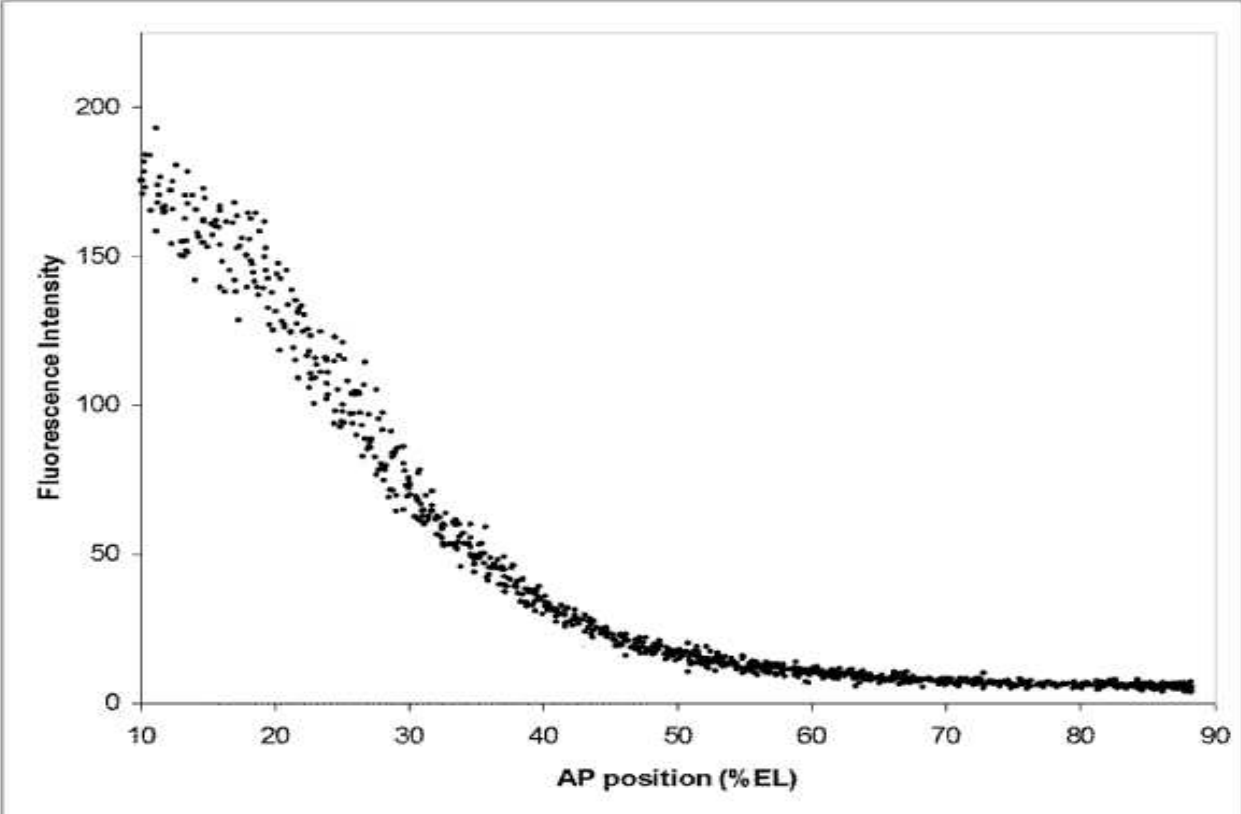
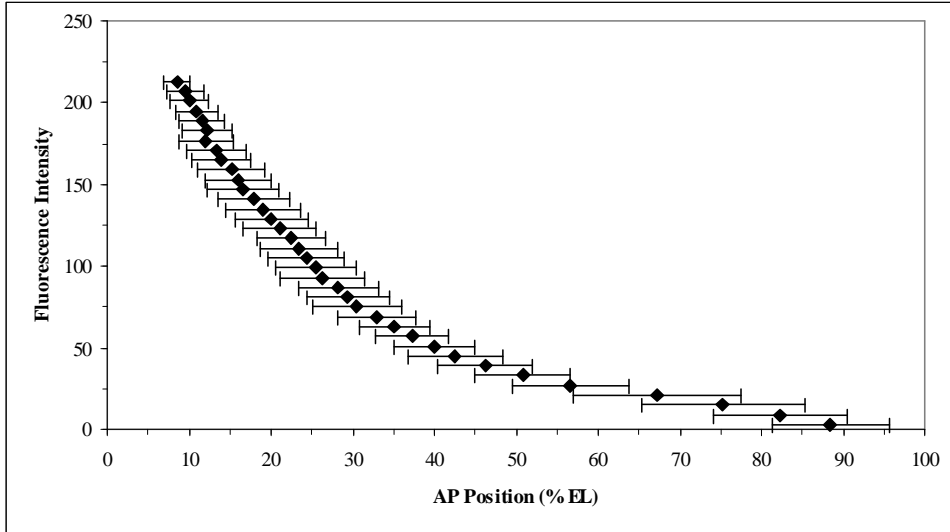
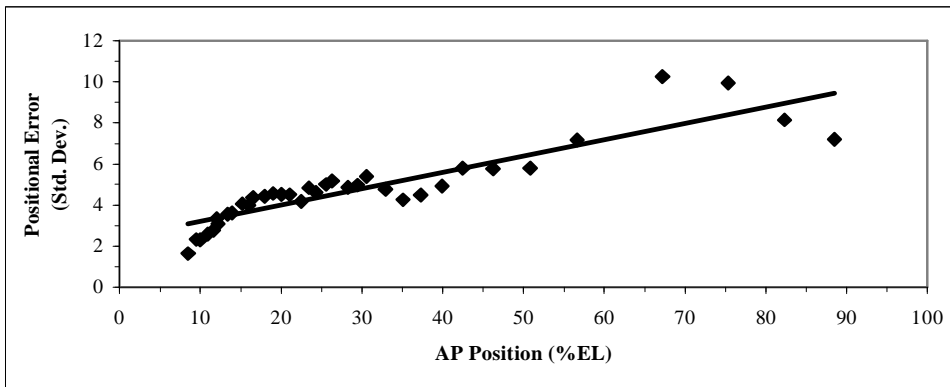


Figure 3

A)



B)



C)

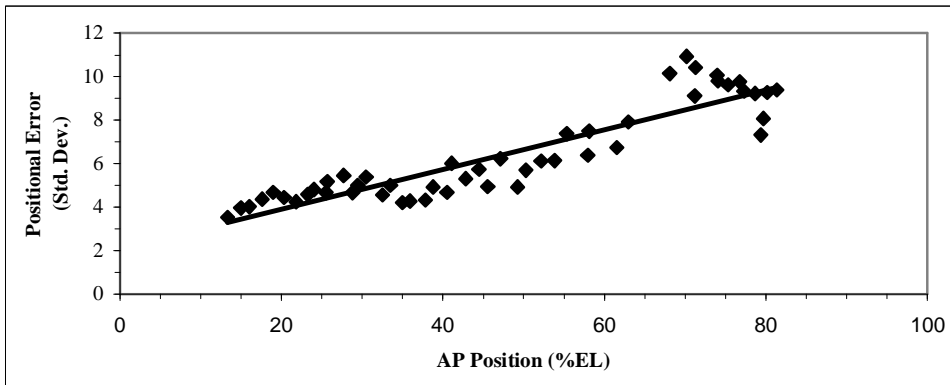
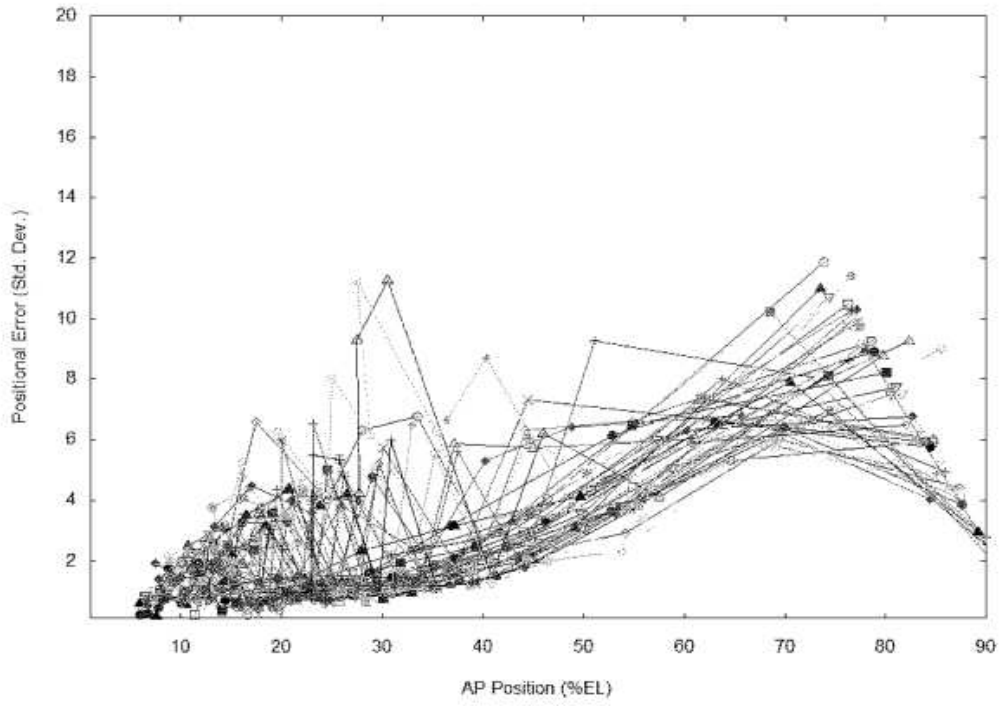


Figure 4

A)



B)

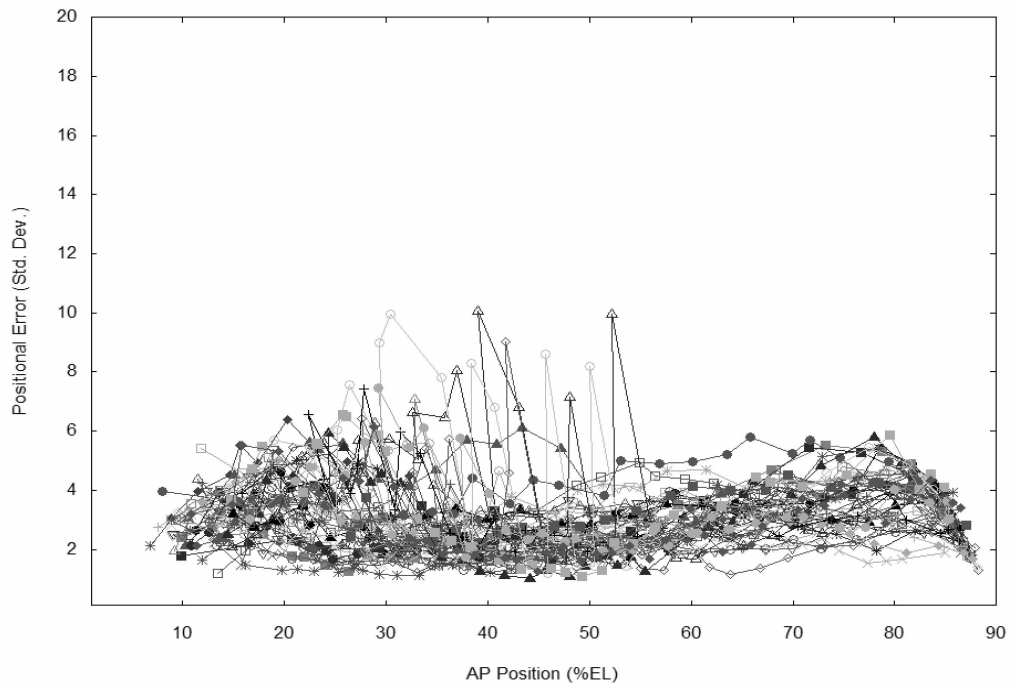


Figure 5

